The EMBO Journal Vol. 22 No. 11 pp. 2658–2667, 2003

A cholesterol-regulated PP2A/HePTP complex with dual specificity ERK1/2 phosphatase activity

Ping-yuan Wang, Pingsheng Liu, Jian Weng, Estelle Sontag[1] and Richard G.W.Anderson[2]

Departments of Cell Biology and [1]Pathology, University of Texas Southwestern Medical Center, Dallas, TX 75390-9039, USA

[2]Corresponding author
e-mail: richard.anderson@utsouthwestern.edu

The acute depletion of membrane cholesterol causes the concentration of pERK1/2 in caveola/raft lipid domains and the cytosol of human fibroblasts to dramatically increase. This increase could be caused by either the activation of MEK-1 or the inhibition of a pERK phosphatase. Here we describe the isolation of a high molecular weight (~440 kDa), cholesterol-regulated pERK phosphatase that dephosphorylates both the phosphotyrosine and the phosphothreonine residues in the activation loop of the enzyme. The dual activity in the complex appears to be due to the combined activities of the serine/threonine phosphatase PP2A and the tyrosine phosphatase HePTP. Acute depletion of cholesterol causes the disassembly of the complex and a concomitant loss of the dual specificity pERK phosphatase activity. The existence of a cholesterol-regulated HePTP/PP2A activity provides a molecular explanation for why ERK activity is sensitive to membrane cholesterol levels, and raises the possibility that ERK plays a role in regulating the traffic of cholesterol to caveolae/rafts and other membranes.

Keywords: cholesterol/ERK/membrane traffic/phosphatase

Introduction

Cells maintain total cholesterol within strict limits by regulating both cholesterol synthesis and the uptake of cholesterol from lipoprotein carriers (Brown and Goldstein, 1997). Regardless of the cholesterol source, however, the cholesterol level of each membrane system must be optimized for the proper function of that membrane. Global cellular cholesterol concentrations appear to be controlled by transcriptional machinery that regulates cholesterol synthesis and uptake (Brown and Goldstein, 1997). Maintaining the correct distribution of cholesterol among membrane systems, on the other hand, appears to depend on membrane traffic, as well as the inter-membrane movement of cytoplasmic transport factors (Maxfield and Wustner, 2002).

The mechanism that cells use to detect cholesterol levels in each membrane system is not known. In the case of the plasma membrane, the sensor must continuously monitor cholesterol and rapidly respond to high or low levels as a result of cholesterol exchange with environmental acceptors. Most likely the sensor is linked to a mechanism for moving cholesterol from sources like the endoplasmic reticulum (ER), lysosomes and lipid stores to sites where it is needed. A cholesterol sensing motif has been identified (Brown and Goldstein, 1997) that is found in several different proteins including NPC1, a molecule that has been genetically linked to the regulation of cholesterol traffic (Garver and Heidenreich, 2002).

One place to look for a cholesterol sensor that regulates cholesterol traffic to the plasma membrane is in plasmalemmal caveolae. This class of lipid domains uses cholesterol as a structural molecule (Rothberg *et al*., 1992). Caveolae have an important function in spatially organizing signal transduction at the cell surface (Anderson, 1998), and cholesterol is critically important for this process. For example, replacing caveolae cholesterol with cholest-4-en-3-one causes relocation of endothelin receptor type A from caveolae to clathrin-coated pits, where it is internalized (Okamoto *et al*., 2000). The presence of cholest-4-en-3-one also attenuates signal transduction by insulin receptors (Gustavsson *et al*., 1999) and platelet-derived growth factor (PDGF) receptors (Liu *et al*., 2000) that are in caveolae. Depletion of caveolae cholesterol also affects signal transduction (Furuchi and Anderson, 1998). Cholesterol depletion of non-caveolae rafts, a related lipid domain, activates the Ras–ERK pathway (Kabouridis *et al*., 2000). The caveolae resident protein caveolin-1 may be involved in supplying cholesterol to caveolae (Uittenbogaard and Smart, 2000).

A device for sensing cholesterol in each membrane compartment must be able to respond rapidly to local fluctuations in cholesterol. One way this might occur is by linking membrane cholesterol levels to the action of a signaling pathway. A key signaling molecule in caveolae that is regulated by cholesterol is ERK1/2 (Furuchi and Anderson, 1998). ERK1/2 belongs to a family of protein serine/threonine kinases that are activated by a variety of growth factors, as well as other extracellular stimuli (Cobb, 1999). ERK1/2 activation depends on MEK, a kinase that phosphorylates both threonine and tyrosine residues located in the activation loop motif TxY of kinase subdomain VIII in ERK1/2 (Zhang *et al*., 1994). Activated ERK1/2 phosphorylates a variety of substrates that are involved in controlling chemotaxis, cell cycle progression and mitogenesis, oncogenic transformation and metastasis, and neuronal differentiation and survival (Cobb, 1999). ERK1/2 activation is reversible, suggesting a role for phosphatases in controlling the level of pERK1/2. The dual specificity phosphatase MKP-3 (Camps *et al*., 2000), as well as the tyrosine phosphatases PTP-SL, HePTP and STEP (Pulido *et al*., 1998), have been implicated in controlling the activity of ERK1 and ERK2. Both sets of enzymes interact with ERK, and the binding of ERK2 to

MKP-3 stimulates its phosphatase activity (Camps *et al*., 1998). The serine/threonine protein phosphatase PP2A may also regulate ERK activation (Sontag *et al*., 1993; Alessi *et al*., 1995). We imagine, therefore, that membrane cholesterol levels could modulate ERK activity in caveolae by regulating either a dual specificity phosphatase or MEK.

A cholesterol-sensitive feedback loop linking kinase activation to phosphatase deactivation of ERK could be used to detect caveolae cholesterol levels. Here we present evidence for the existence of a novel, dual specificity ERK phosphatase activity that depends on the combinatorial interaction between the HePTP family of tyrosine phosphatases and the threonine phosphatase PP2A. Acute depletion of membrane cholesterol causes the HePTP/PP2A complex to disassemble, leading to an increase in pERK.

Results

Cholesterol-regulated dephosphorylation of pERK

The increased level of pERK1/2 found in the caveolae/rafts fraction and cytosol following cholesterol depletion could be caused by either stimulating MEK-1 kinase or inhibiting a pERK1/2 phosphatase. To distinguish between these two possibilities, normal human fibroblasts were grown in 10% serum to maintain growth factor receptor activity (Figure 1A). The cells were incubated for 15 min in the presence of various concentrations of PDGF, with (lanes 5–8) or without (lanes 1–4) the addition of the MEK-1 inhibitor PD98059, and the samples were assayed for cellular pERK by immunoblotting with an antibody that only recognizes pERK when both the threonine and tyrosine are phosphorylated (α-pT&pY ERK1/2 IgG). Cells not exposed to PDGF contained pERK (Figure 1A, lane 1) but the level of pERK was markedly reduced in cells exposed to PD98059 (lane 5). This suggests that growth factors in the serum maintain pERK levels by stimulating MEK-1 and that blocking MEK-1 allow an endogenous pERK phosphatase to dephosphorylate pERK. The same result was obtained when cells were stimulated with different concentrations of PDGF (Figure 1A, compare lanes 2–4 with 6–8). PD98059 had no effect on PDGF-stimulated tyrosine phosphorylation of proteins in the 180 kDa region of the gel (Figure 1A, PY, 180 kDa). Based on these results, we next incubated cells in the presence of the MEK-1 inhibitor PD98059 for 10 min before adding the cholesterol adsorbing resin methyl-β-cyclodextrin (CD) for 15 min at 37°C (Figure 1B) to deplete cell cholesterol. The cells were then fractionated and the relative amount of pERK in either the caveolae/rafts fraction (Figure 1B, lanes 1–3) or the cytosol (lanes 4–6) was detected by immunoblotting. Under these conditions, CD treatment caused a marked increase in the amount of pERK in both caveolae/rafts (Figure 1B, compare lanes 1 and 2) and cytosol (lanes 4 and 5) fractions. We conclude that the increase in the amount of pERK1/2 was due to the inhibition of a pERK phosphatase. Indeed, when the tyrosine phosphatase inhibitor orthovanadate was substituted for CD, we also saw a dramatic increase in the amount of pERK in both the caveolae/rafts fraction (Figure 1B, lane 3) and the cytosol

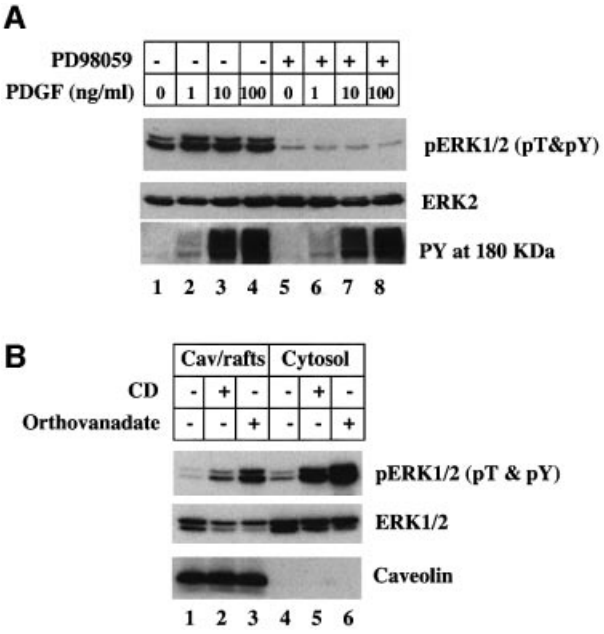

Fig. 1. Cytosol and the caveolae/rafts membrane fraction contain an orthovanadate-sensitive, cholesterol-sensitive pERK phosphatase activity. Normal human fibroblasts were grown in DMEM containing 10% fetal bovine serum (FBS). (**A**) Cells were incubated for 10 min in the presence or absence of 20 μM PD98059 before the indicated concentration of PDGF was added and the cells were incubated for an additional 15 min. The whole-cell lysate was processed to detect dual phosphorylated pERK1/2 (pT&pY), ERK2 and phosphotyrosine containing proteins in the 180 kDa region of the gel (PY, 180 kDa) by immunoblotting. (**B**) Cells were incubated for 10 min in the presence of 20 μM PD98059 to inhibit MEK-1. Either 1% CD or 1 mM sodium orthovanadate was then added to the medium and the cells further incubated 15 min at 37°C. The cells were washed and the cytosol and caveolae/rafts (Cav/rafts) fractions were prepared. Equal amounts of the caveolae/rafts and cytosol fraction (17 μg of protein) were processed for immunoblotting to detect dual phosphorylated pERK1/2 (pT&pY), ERK2 and caveolin-1. This figure is representative of three separate experiments.

(lane 6). Thirty minutes of CD treatment was required to reach maximum levels of pERK (data not shown).

The major pERK phosphatases that have been identified are soluble enzymes. Therefore, a strategy was developed to identify the cholesterol regulated pERK phosphatase using cytosol as a source and a commercial pERK2–glutathione *S*-transferase (GST) fusion peptide as the substrate. We first tested the effects of different CD concentrations on the level of endogenous cytosolic pERK in two different cells, normal human fibroblasts (Figure 2A, lanes 1–7) and HeLa cells (lanes 8–14). Exposure to as little as 0.5% CD for 15 min caused an increase in the amount of pERK1/2 detected by immunoblotting the lysates from both cell types (Figure 2A, compare lane 1 with 2, and lane 8 with 9). Mixing cholesterol with the CD markedly suppressed the level of pERK (Figure 2A, lanes 5–7 and 12–14). We next assayed the endogenous pERK phosphatase activity in fibroblast cytosol using pERK2–GST as the substrate and α-pT&pY ERK1/2 IgG to detect dephosphorylation (Figure 2B). Cells were exposed to 10 ng/ml of PDGF for 30 min, which stimulates phosphorylation of endogenous ERK1/2, so that we could monitor endogenous pERK levels. Cytosol from PDGF-treated cells (Figure 2B, lane 2) very effectively dephosphorylated pERK2–GST.

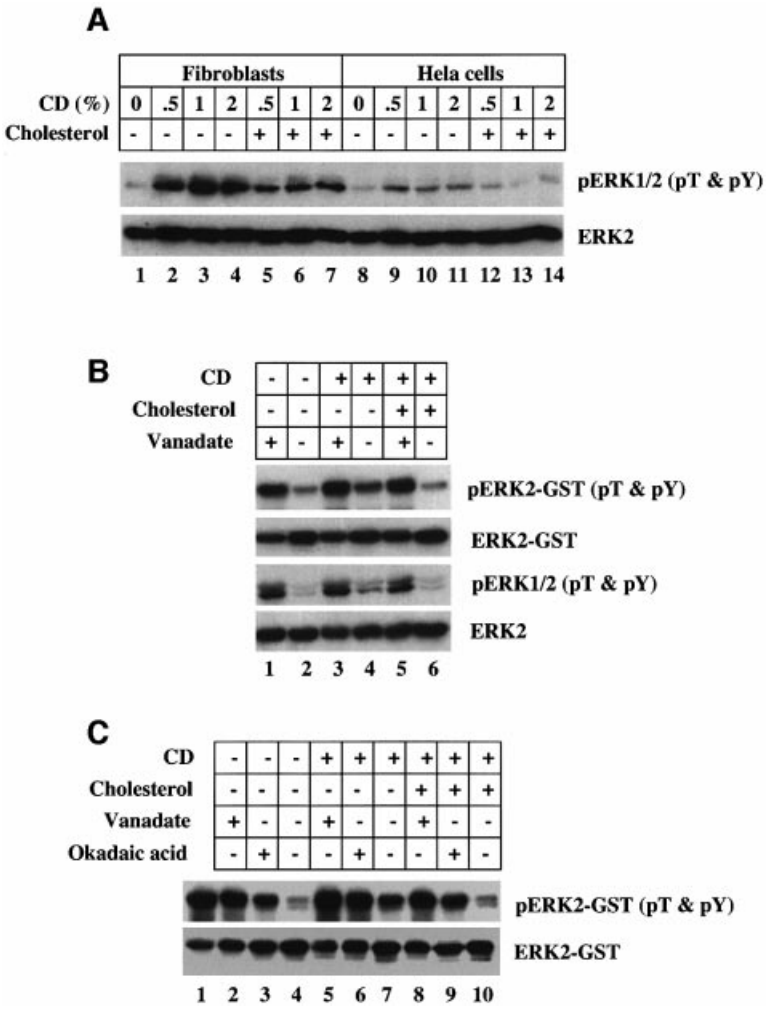

Fig. 2. An orthovanadate and okadaic acid sensitive cytosolic pERK phophatase is inhibited by acute depletion of cholesterol. (**A**) Normal human fibroblasts and HeLa cells grown in DMEM plus 10% FBS were pre-incubated in the presence of 20 μM PD98059 for 10 min at 37°C before the indicated concentration of CD plus or minus 100 μg/ml of cholesterol was added to the medium and the cells incubated an additional 15 min at 37°C. Equal amounts of whole-cell lysate were processed for immunoblotting to detect dual phosphorylated pERK1/2 with α-pT&pY ERK1/2 IgG and ERK2 with α-ERK1/2 IgG. (**B**) Normal human fibroblasts grown in DMEM with 10% FBS were incubated in the presence of 10 ng/ml PDGF to stimulate phosphorylation of endogenous ERK. At the same time, the cells were incubated in the presence or absence of 1% CD plus or minus the addition of 100 μg/ml cholesterol for 30 min at 37°C. Cytosol (30 μg) was prepared and mixed with 100 ng of pERK2–GST in the presence or absence of 1 mM othovanadate and incubated for 30 min at 30°C before 20 μl of glutathione beads were added to remove the ERK2–GST as described. The ERK2–GST and the cytosol were processed for immunoblotting to detect the amount of pERK2–GST on the beads and pERK in the cytosol with α-pT&pY ERK1/2 IgG and the amount of ERK2–GST and ERK2 in the cytosol with α-ERK2 IgG. (**C**) The same procedure as described in (B) except the phosphatase reaction was carried out in the presence or absence of either 100 nM okadaic acid or 1 mM orthovanadate for 30 min at 30°C. This figure is representative of three separate experiments.

Markedly less dephosphorylation was detected when the cytosol from cholesterol-depleted cells was used (Figure 2B, lane 4). Pre-mixing the CD with cholesterol abolished this effect (Figure 2B, lane 6). Orthovanadate was more effective than cholesterol depletion at reducing the pERK2–GST phosphatase activity (Figure 2B, compare lanes 1 and 4). Immunoblots of endogenous pERK (pERK1/2) showed that the phosphorylation state of endogenous ERK1/2 paralleled that of pERK2–GST. Finally, we tested the effect of the serine/threonine phosphatase inhibitor, okadaic acid (Figure 2C). Compared with untreated pERK2–GST (Figure 2C, lane 1), the cytosol from control cells effectively dephosphorylated pERK2–GST (lane 4). Okadaic acid (Figure 2C, lane 3) and orthovanadate (lane 2) inhibited dephosphorylation. Cholesterol depletion followed by treatment of the cytosol with orthovanadate (Figure 2C, lane 5) or okadaic acid (lane 6) was more effective than either alone. We conclude that the cytosol contains a pERK phosphatase that removes phosphate from both threonine and tyrosine, and is inhibited either by depleting cells of cholesterol or by exposing the isolated cytosol to orthovanadate or okadaic acid.

The same phosphatase activity appears to be present in both human fibroblasts and HeLa cells. Therefore, we used column chromatography to enrich for the cholesterol-regulated pERK phosphatase activity detected in HeLa cells, because these cells grow quickly, are easily transfected and are a more abundant source of cytosol (Figure 3A). After multiple trials, we settled on a two-column protocol taking the cytosol fractions eluted from a MonoQ 5/5 column between 350 and 380 mM NaCl, and

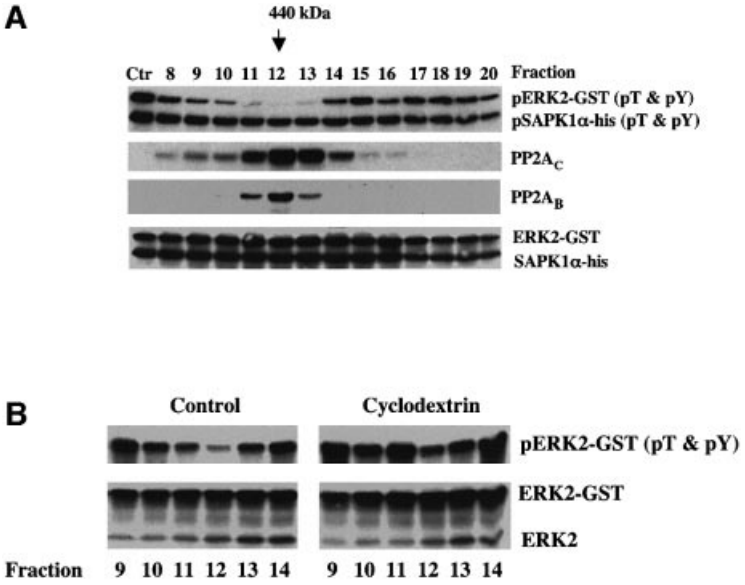

Fig. 3. The orthovanadate-, okadaic acid-, cholesterol-sensitive pERK phosphatase activity in the cytosol is associated with a high molecular weight complex. (**A**) HeLa cells were grown in DMEM plus 10% FBS before cytosol was isolated and subjected to the fractionation protocol described. Equal volumes (50 μl) of fractions 8–20 from the Superdex 200 column were mixed with 50 ng of pERK2–GST and 50 ng of pSAPK1α-his and incubated for 1 h at 30°C before processing each sample for immunoblotting the indicated antigen. pERK2–GST and pSAPK1α-his were blotted with an antibody that only recognizes the dual phosphorylated form. Ctr is untreated pERK2–GST and pSAPK1α-his. (**B**) HeLa cells were grown as described and incubated for 1 h in the presence or absence of 1% CD. The cells were homogenized and the cytosol fractions separated and assayed for dual specificity phosphatase activity as described in (A). Equal volumes of fractions 9–14 were used for the pERK2–GST dephosphorylation assay. This figure is representative of three separate experiments.

separating this material on a Superdex 200 gel filtration column. Fractions 8–20 (1 ml each) were assayed for phosphatase activity using both pERK2–GST and pSAPK1α as substrates. Compared with untreated pERK2–GST (Figure 3A, lane Ctr), fractions 11–13 very effectively dephosphorylated pERK2–GST. These same fractions did not dephosphorylate pSAPKα, indicating that the activity is specific for ERK MAP kinase. The detected activity had an apparent molecular weight of ~440 000 (arrow). These same fractions in cholesterol-depleted cells had markedly less pERK2–GST phosphatase activity (Figure 3B, compare fraction 12 from CD-treated and control cells), even though the amount of ERK2 in each fraction remained unchanged. Since PP2A has previously been implicated in the dephosphorylation of pERK (Sontag *et al*., 1993), we immunoblotted each fraction with an antibody that recognizes either the C subunit (PP2A$_C$) or the B subunit (PP2A$_B$) of PP2A (Figure 3A), and found that both subunits co-fractionated with the cholesterol-regulated pERK phosphatase activity.

Cholesterol-regulated pERK phosphatase contains PP2A

We used immunodepletion to further establish that the phosphatase activity we have detected contains PP2A (Figure 4A). Cytosol was fractionated on MonoQ and Superdex 200 columns and fractions 10–13 were pooled. Samples of these fractions were incubated in the presence of either an irrelevant mAb IgG or an mAb directed against the C subunit of PP2A (α-PP2A$_C$ IgG) before adding pre-blocked protein G-coated beads and centrifuging to remove the beads. Either the supernatant fraction (Figure 4A, lanes 2–7) or the beads (lanes 8–13) were then assayed for phosphatase activity by immunoblotting pERK2–GST with α-pT&pY ERK1/2 IgG. Compared with non-immune IgG [pERK2–GST (pT&pY); Figure 4A, lane 8], the α-PP2A$_C$ IgG pulled down strong pERK phosphatase activity (Figure 4A, compare lanes 1 and 11), which was accompanied by a loss of activity from the supernatant fraction (compare lanes 2 and 5). This activity was markedly inhibited by both orthovanadate (Figure 4A, lane 12) and okadaic acid (lane 13), indicating that the phosphatase on the beads has the properties of the cholesterol-regulated phosphatase. Antibodies are available that detect either the phosphothreonine or the phosphotyrosine on pERK2–GST. These antibodies showed that the phosphatase activity in the PP2A$_C$ pull-down was able to dephosphorylate both the threonine (Figure 4A, lane 11, pERK2–GST pT) and the tyrosine (lane 11, pERK2–GST pY) residues on pERK2–GST. Moreover, both phosphatase activities were sensitive to orthovanadate (Figure 4A, lane 12) and okadaic acid (lane 13).

We further characterized the cholesterol-regulated PP2A complex by comparing its activity with the activity of a commercially purified PP2A using the same buffer conditions (Figure 4B). As expected, the commercial PP2A A/C dimer very effectively dephosphorylated the pT in pERK2–GST (pERK2–GST, pT) but did not dephosphorylate the pY (pERK2–GST, pY). The pT phosphatase activity was not sensitive to orthovanadate (Figure 4B, lane 3). Conversely, the cholesterol-regulated PP2A complex that was pulled down from the Superdex column fractions with α-PP2A$_C$ IgG was not sensitive to orthovanadate when it was assayed for its ability to dephosphorylate the commercial PP2A substrate K-R-pT-I-R-R (Figure 4C). These results suggest a molecular component of the isolated PP2A complex confers

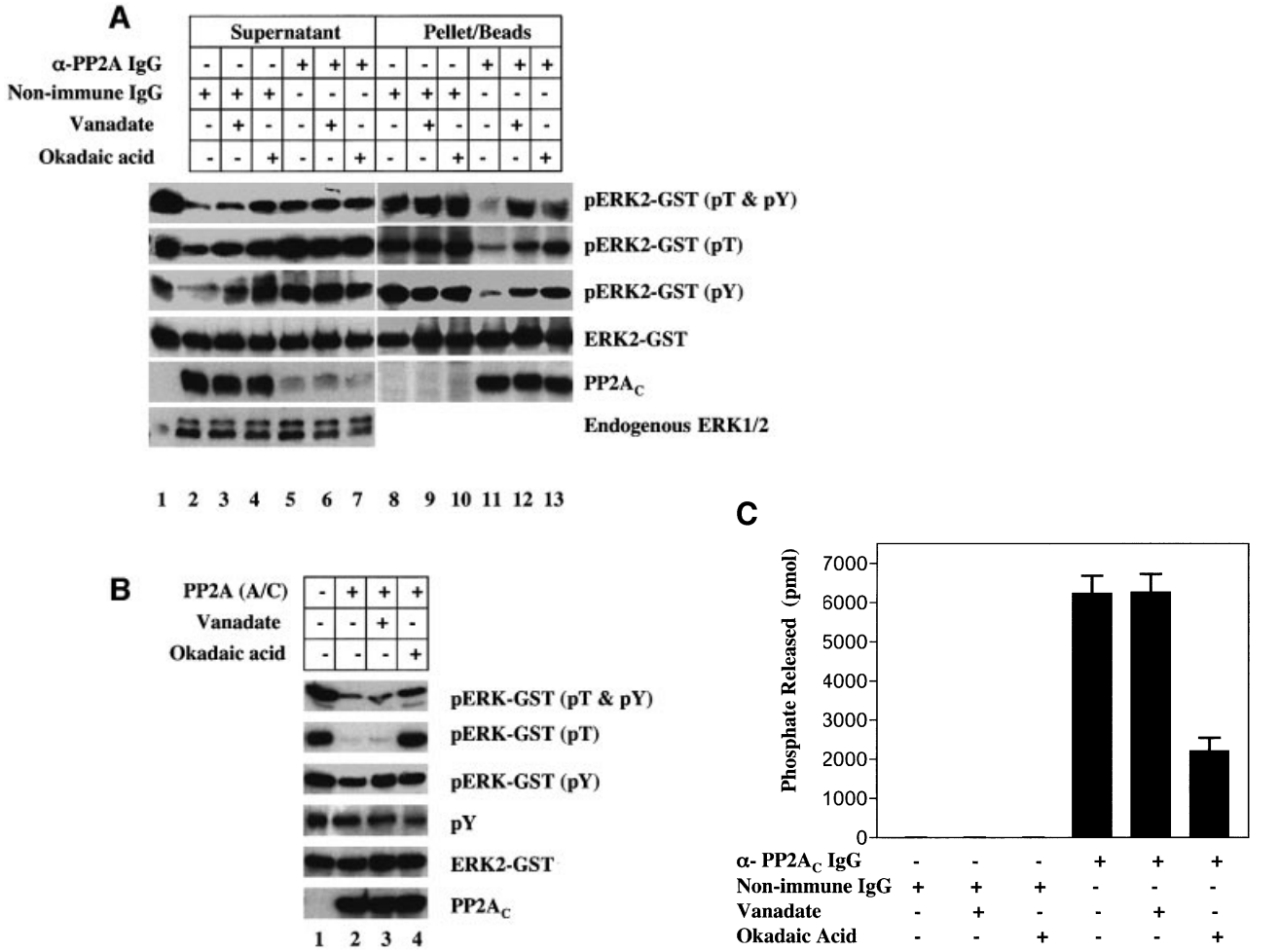

Fig. 4. α-PP2A$_C$ IgG pulls down a tyrosine and threonine pERK phosphatase activity. (**A**) HeLa cells were grown and fractionated as described in Figure 3. Fractions 10–13 from the Superdex column were pooled and processed for immuno-isolating the C subunit of PP2A as described. The pERK phosphatase activity in both the supernatant fraction and the bead pellet was measured as described using 1 mM orthovanadate or 3 nM okadaic acid as indicated at 30°C. Incubation times for the reaction were 1 h for the supernatant fraction and 3 h for the beads. Each sample was processed for immunoblotting the indicated antigen. (**B**) The purified, dimerized PP2A core enzyme was tested for pT and pY activity on the pERK2–GST substrate as described. The samples were incubated for 1 h at 30°C and processed for immunoblotting. (**C**) PP2A$_C$ immuno-isolated from fractions 11–13 of the Superdex column were tested for phosphatase activity using the substrate K-R-pT-I-R-R as described. Phosphatase reaction time was 1 h at 30°C. This figure is representative of three to eight separate experiments.

substrate-specific orthovanadate sensitivity to the dephosphorylation of pERK.

Cholesterol-regulated PP2A complex contains HePTP

These results indicate that the PP2A in the complex we have isolated is not responsible for dephosphorylating the pY residue in pERK. A detailed *in vitro* kinetic analysis has shown that the most likely pY phosphatase to act on pERK is either MKP-3 or a member of the HePTP family of tyrosine phosphatases (Zhou *et al*., 2002). We discounted MKP-3 because it is a dual specificity phosphatase that is not sensitive to okadaic acid, and focused on the possibility that the tyrosine phosphatase activity in the complex was due to HePTP. Owing to the unavailability of a suitable α-HePTP IgG, we expressed in HeLa cells a cDNA coding for hemagglutinin (HA)-tagged HePTP and used immunoblotting to determine whether expressed HePTP-HA co-fractionated with the high molecular weight PP2A complex (Figure 5A). When the eluate from the MonoQ column was separated on the Superdex 200, HePTP-HA and the endogenous PP2A were in the same fraction. We conclude that the high molecular weight complex with phosphatase activity contains both HePTP and PP2A.

We used immunoprecipitation to determine whether the PP2A and HePTP-HA in the fractions were part of the same complex (Figure 5B and C). HePTP-HA was expressed in HeLa cells and the cytosol fractionated on MonoQ and Superdex 200. Fractions 10–13 from the Superdex 200 column were pooled and processed to immunopurify either PP2A (Figure 5B) or HePTP-HA (Figure 5C). The immunoprecipitates were then separated by gel electrophoresis and immunoblotted to detect PP2A and HePTP-HA. mAb α-PP2A$_C$ IgG immunoprecipitated both PP2A$_C$ and HePTP-HA (Figure 5B, lane 4) and the non-immune IgG did not pull down either one (Figure 5B, lane 3). Likewise, pAb HA IgG pulled down both PP2A

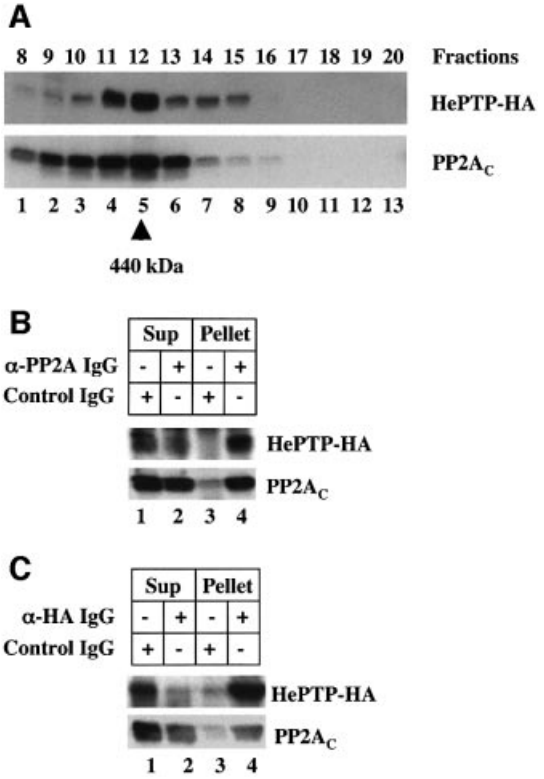

Fig. 5. The high molecular weight pERK phosphatase complex contains HePTP. (**A**) HeLa cells were transfected with a cDNA coding for HePTP-HA. The cytosol was prepared and fractionated as described. Equal volumes of fractions 8–20 were separated by gel electrophoresis and immunoblotted for HePTP-HA and PP2A$_C$. (**B**) HeLa cells were transfected with cDNA for HePTP-HA and the cytosol fractionated as described. PP2A$_C$ was immuno-isolated from fractions 10–13 and processed for immunoblotting of both HePTP-HA and PP2A$_C$. (**C**) HeLa cells were transfected with cDNA for HePTP-HA and the cytosol fractionated as described. HePTP-HA was immuno-isolated from fractions 10–13 and processed for immunoblotting of both HePTP-HA and PP2A$_C$. This figure is representative of three separate experiments.

and HePTP-HA (Figure 5C, lane 4). These results indicate that the HePTP-HA and PP2A in the high molecular weight complex are physically linked.

An important final test was to determine whether pAb HA IgG could immunoprecipitate the pT-pY pERK phosphatase activity. HeLa cells were transfected with the HePTP-HA cDNA and fractions 10–13 from the Superdex column were pooled. The pAb HA IgG immunoprecipitates from these fractions were tested for pY and pT pERK2–GST phosphatase activity (Figure 6, lanes 5–7). Immunoblotting with specific antibodies showed that compared with untreated pERK2–GST (Figure 6, lane 1), the immunoprecipitate dephosphorylated both the tyrosine (pY) and the threonine (pT) residues on pERK2–GST (lane 5). Moreover, these two phosphatase activities were markedly inhibited by both orthovanadate (Figure 6, lane 6) and okadaic acid (lane 7). The pAb HA did not immunoprecipitate any activity from untransfected cells (data not shown). Therefore, both the pT and the pY phosphatase activities in the complex can be accounted for by the combined activity of PP2A and HePTP.

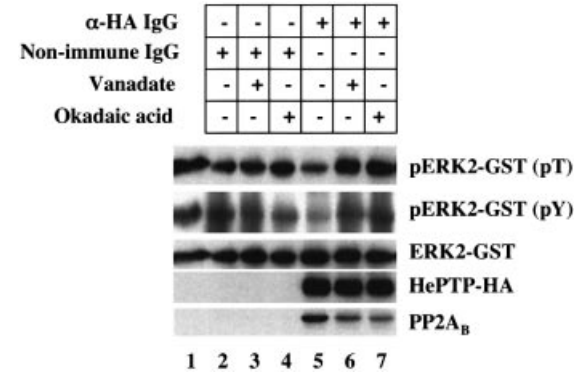

Fig. 6. A complex of HePTP/PP2A in the high molecular weight fraction can dephosphorylate both pY and pT in pERK. HeLa cells were transfected with the cDNA for HePTP-HA and fractionated as described. Fractions 10–13 from the Superdex column were pooled and the HePTP-HA was immuno-isolated using beads coated with either non-immune IgG or α-HA IgG. Each sample was assayed for phosphatase activity using antibodies specific for pT and pY pERK2–GST as described in Figure 4 using a 3 h incubation at 30°C and 1 mM orthovanadate or 3 nM okadaic acid. Lane 1 is an untreated sample of the pERK2–GST. This figure is representative of three separate experiments.

Mechanism of cholesterol regulation

Our initial fractionation trials (Figure 3B) indicated that the high molecular weight pERK phosphatase activity was markedly reduced in cholesterol-depleted cells. One explanation for this result is that cholesterol regulates the interaction between PP2A and HePTP. We used immunoprecipitation to determine whether lowering cell cholesterol affected the interaction between PP2A and HePTP (Figure 7A). Transiently transfected HeLa cells expressing HA-HePTP were incubated for 1 h in the presence or absence of 1% CD. The cytosol fraction was prepared and processed to immunoprecipitate the phosphatase complex using either α-HA IgG (Figure 7A, lanes 2, 4, 6 and 8) or a non-immune IgG (lanes 1, 3, 5 and 7). The supernatant and pellet fractions were separated and tested for the presence of HA-HePTP and both the C and the A subunit of PP2A. The α-HA IgG immunoprecipitate from the cytosol of control cells contained HA-HePTP as well as the two PP2A subunits (Figure 7A, lane 4), which is in agreement with the results shown in Figures 5 and 6. The two PP2A subunits were not present in the immunoprecipitate prepared from the cholesterol-depleted cells (Figure 7A, lane 8), indicating that CD treatment had disrupted the complex. The non-immune IgG did not pull down significant amounts of either HA-HePTP or PP2A (Figure 7A, lanes 3 and 7). A second test utilized blue native gel electrophoresis (Figure 7B). This method allows the separation of high molecular weight complexes under non-denaturing conditions without immunoprecipitation (Yang *et al*., 2002). We loaded 90 μg of cytosol protein from untreated cells, separated the sample by electrophoresis in 6–16% gels and immunoblotted with an α-HA IgG (Figure 7B, lane 1). A prominent band was present in the region of the gel where the 440 kDa marker migrated (Figure 7B, arrow A). Three less intense bands were also detected, which migrated at lower molecular weights. The high molecular weight band had the same apparent size as the phosphatase complex we isolated from the Superdex 200 column (Figure 3A). Importantly, when we separated

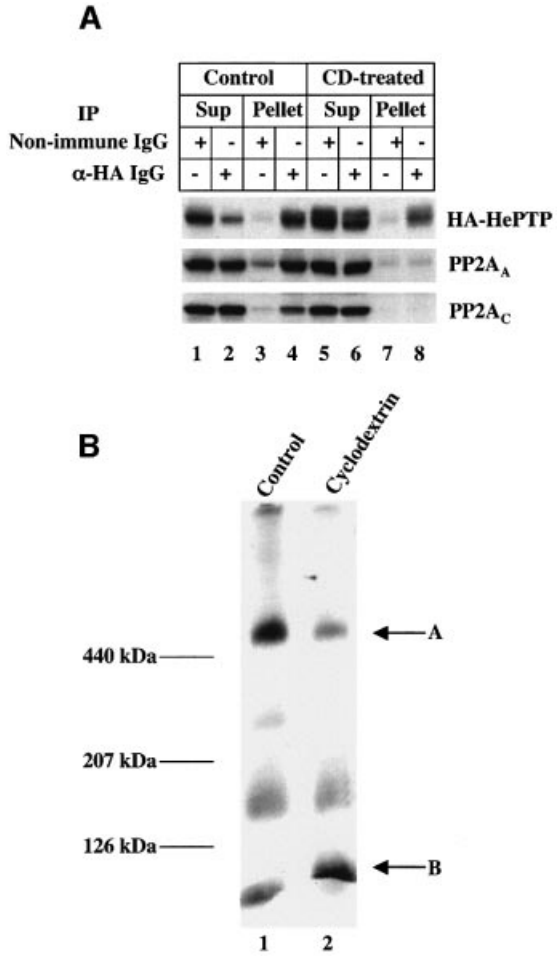

Fig. 7. Cholesterol depletion causes the disassembly of the HePTP/PP2A complex. (**A**) HeLa cells were transfected with the cDNA for HePTP-HA. Cells were incubated in the presence or absence of 1% CD for 1 h before preparing cytosol and immuno-isolating HePTP-HA using beads coated with either non-immune or α-HA IgG. The supernatant and the beads were then processed for immunoblotting using antibodies directed against either HePTP-HA or the A (PP2A$_A$) and the C (PP2A$_C$) subunit of PP2A. (**B**) HeLa cells were transfected with the cDNA for HePTP and grown in DMEM plus 10% FBS. The cells were incubated in the presence or absence of 1% CD for 1 h before preparing cytosol. The cytosol (90 μg/lane) from each cell was then separated using blue native gel electrophoresis as described. The gels were processed for immunoblotting with α-HA antibody. This figure is representative of three to four separate experiments.

a sample of cytosol from cholesterol-depleted cells, the intensity of the HA-HePTP high molecular weight band was markedly reduced (Figure 7B, arrow A, lane 2) and the intensity of the lowest molecular weight band (<120 kDa) was increased (Figure 7B, arrow B, lane 2). The dissociation of the two enzymes was not a consequence of ERK1/2 activation, as the HePTP/PP2A complex remained intact in cells exposed to PDGF (data not shown). These results suggest that cholesterol regulates the ERK dual specificity activity we have isolated by controlling the interaction between PP2A and HePTP.

Discussion

We have identified a novel, high molecular weight complex that can dephosphorylate both the pT and the pY in pERK, but not in pSAPK. The combined phosphatase activities appear to depend on the presence of both PP2A and HePTP in the complex. Most likely PP2A dephosphorylates the threonine in the activation loop, while HePTP dephosphorylates the tyrosine. Both enzymes have previously been implicated in the control of ERK activity. For example, Sontag and colleagues showed that SV40 small tumor antigen activates ERK1/2 by binding to and inactivating PP2A, resulting in cell proliferation (Sontag *et al*., 1993). ERK2 has been found to be a specific substrate for HePTP (Pettiford and Herbst, 2000), which appears to depend on an interaction between ERK2 and a 16 amino acid motif in HePTP called the KIM domain (Pulido *et al*., 1998). The KIM domain is found in the two related phosphatases, STEP and PCPTP (PTP-SL) (Shiozuka *et al*., 1995). Our result suggests that cholesterol regulates the assembly of these two phosphatases into a high molecular weight complex that acts coordinately to control the activation state of ERK.

The HePTP/PP2A complex

PP2A is a serine/threonine phosphatase that is involved in regulating a wide variety of signaling pathways (for a review see Sontag, 2001). The specific target of the holoenzyme appears to depend on the type of regulatory subunit that is associated with the common catalytic and scaffolding subunits. The molecular weight of the trimeric complex is ~150 000. One of the hallmarks of the enzyme activity is its exquisite sensitivity to okadaic acid but insensitivity to orthovanadate. HePTP is a 40 kDa, orthovanadate-sensitive tyrosine phosphatase originally discovered in lymphocytes (Zanke *et al*., 1992), but also expressed in other tissues (Pettiford and Herbst, 2000). Lymphocytes from mice that lack this enzyme show enhanced ERK activation in response to various stimuli (Gronda *et al*., 2001), suggesting that it is a physiological regulator of ERK activity. Our results indicate that a subpopulation of HePTP and PP2A in cells is physically associated in an ~440 kDa complex. Immunoblotting showed that the two enzymes co-purify with the high molecular weight cholesterol-regulated ERK phosphatase activity. Immunoprecipitation of any of the PP2A subunits or of HePTP from this fraction co-precipitated the entire complex, and these precipitates contain the dual specific ERK phosphatase activity. The size of this complex appears to be larger than the aggregate molecular weight of the two enzymes, which suggests that it contains additional as yet unidentified proteins.

The enzymic properties of the HePTP/PP2A complex are uniquely different from those of the component enzymes. PP2A is insensitive to orthovanadate, while tyrosine phosphatases like HePTP are not inhibited by okadaic acid. The pT and pY phosphatase activity of HePTP/PP2A, by contrast, is sensitive to both inhibitors, but only when pERK is the substrate. This suggests that within the complex the two enzymes work cooperatively on pERK1/2. Recent kinetic studies using purified enzymes have shown that HePTP efficiently dephosphorylates both ERK2/pTpY and ERK2/pY, while dephosphorylation by PP2A is 22 times slower for ERK2/pTpY compared with ERK2/pT (Zhou *et al*., 2002). The PP2A in HePTP/PP2A complex may be able to engage pERK but not efficiently remove the phosphate from threonine until the tyrosine is dephosphorylated.

Simple kinetics, however, cannot explain why the HePTP activity in the complex is inhibited by okadaic acid. We imagine in this case that the HePTP in the complex cannot engage the pY without a conformational change in pERK that only occurs when the threonine is dephosphorylated. Initially, PP2A slowly dephosphorylates pERK, which allows HePTP to engage and dephosphoryalte pY. This, in turn, stimulates more dephosphorylation of threonine and so forth. At this point we can only speculate about the molecular basis of the cooperative behavior of the two enzymes in the complex. Nevertheless, this behavior emphasizes that the dual specificity phosphatase activity displayed by the complex is a gain of function, acquired as a result of specific interactions between the two enzymes, other molecules in the complex and the substrate.

HePTP may not be the only member of this tyrosine phosphatase family that can associate with PP2A. The homology between HePTP, STEP and PCPTP is very high, particularly in the region containing the KIM domain, the three regulatory threonine and serine residues and the catalytic domain (Saxena *et al*., 1999). Thus, we cannot rule out the possibility that the HA-HePTP we expressed in the HeLa cells used for these experiments displaced a naturally occurring, endogenous isoform of this family of tyrosine phosphatases that normally makes up the complex.

Cholesterol-regulated ERK phosphatase activity

The original goal of this study was to determine why lowering membrane cholesterol, either by removing the sterol with CD (Furuchi and Anderson, 1998) or sequestering it with filipin (Kabouridis *et al*., 2000), stimulates ERK activation. There were two possibilities: lowering caveolae cholesterol either stimulates the phosphorylation of ERK or it inhibits a pERK phosphatase that normally acts to control the steady-state level of pERK. We found that PD98059 did not inhibit ERK activation, but that both orthovanadate and okadaic acid were as effective as cholesterol depletion at causing an increase in caveolae pERK. The sensitivity to 3 nM okadaic acid ruled out MKP-3 (Groom *et al*., 1996), a dual specificity phosphatase that is highly specific for pERK (Zhou *et al*., 2002). Therefore, the ability of orthovanadate to mimic cholesterol depletion was the critical tool we needed to link the pERK phosphatase activity in caveolae to the high molecular weight complex we could isolate from the cytosol. Most likely it is the KIM domain in HePTP that is responsible for targeting the HePTP/PP2A complex in the cytoplasm to the pERK in caveolae. HePTP/PP2A may be responsible for the unidentified pERK tyrosine phosphatase activity previously detected in Swiss 3T3 fibroblasts (Alessi *et al*., 1995).

Cholesterol appears to regulate HePTP/PP2A activity by controlling the presence of HePTP and PP2A in the high molecular weight complex. Acute depletion of membrane cholesterol concomitantly caused loss of enzyme activity from the high molecular weight fraction (Figure 3B), loss of PP2A from the HePTP immunoprecipitate (Figure 7A) and loss of HePTP from the high molecular weight band on blue native gels (Figure 7B). Without their partner, each enzyme individually apparently cannot coordinately inactivate pERK. The function of cholesterol may be to promote assembly of the two enzymes, possibly through the action of a cholesterol-binding protein in the complex that contains a star-related lipid-transfer (START) domain (Ponting and Aravind, 1999). Alternatively, cholesterol may indirectly control assembly by modulating other signaling pathways. For example, there are two sites in HePTP with the consensus amino acid sequence for ERK (Pulido *et al*., 1998) and cAMP-dependent PKA (Saxena *et al*., 1999) phosphorylation, respectively. Cholesterol might regulate the assembly of the HePTP/PP2A complex by modulating the activity of these two kinases.

ERK and cholesterol traffic

The identification of HePTP/PP2A as a cholesterol-regulated ERK phosphatase with dual specificity activity provides a molecular explanation for how fluctuations in membrane cholesterol can affect the level of pERK in both caveolae and the cell cytoplasm. Recent studies have established a link between pERK1/2, phosphorylation of SREPB on Ser117 and the regulation of LDL receptor promoter activity by PDGF and insulin (Roth *et al*., 2000). The identification of HePTP/PP2A raises the possibility that a linkage also exists between pERK and intracellular cholesterol traffic.

Cholesterol appears to move among intracellular membranes by both diffusible sterol carrier proteins like the steroidogenic acute regulatory protein (StAR) and by vesicular traffic (Maxfield and Wustner, 2002). It is often hard to determine the contribution of each mode of transport. While cholesterol clearly can travel between the Golgi apparatus and endosomal elements, there also is a direct pathway between the endoplasmic reticulum and caveolae (Smart *et al*., 1996; Fielding and Fielding, 1997). In fact, cholesterol can move bi-directly between the plasma membrane and the ER (Lange, 1994). Efflux of ER cholesterol to caveolae (Smart *et al*., 1996) and influx of membrane cholesterol to ER (Lange, 1994) are both inhibited by pharmacological concentrations of progesterone, which suggests a common mechanism of transport that may involve caveolin-1. Caveolin-1 binds cholesterol (Murata *et al*., 1995) and accelerates the transport of newly synthesized cholesterol to the plasma membrane (Smart *et al*., 1996). Progesterone causes caveolin-1 to accumulate in internal membranes (Smart *et al*., 1996), resulting in the selective depletion of caveolae cholesterol (Furuchi and Anderson, 1998). Apolipoprotein A-I has been found to induce the translocation of caveolin-1 along with cholesterol and phospholipids to the cytosol (Ito *et al*., 2002). Finally, a cytoplasmic pool of caveolin-1 in a complex with chaperones and annexin II has been implicated in caveolae–ER cholesterol transport (Uittenbogaard *et al*., 2002). Therefore, the ERK1/2 in caveolae is spatially restricted to a region of plasma membrane that experiences dynamic fluctuations in cholesterol (Fielding and Fielding, 1997) and, therefore, is optimally positioned to sense changes in membrane cholesterol.

A potential target of pERK is NPC1. Niemann–Pick type C disease is an autosomal recessive lipid storage disorder that is caused in part by a defect in intracellular cholesterol transport. Defects in two different genes (for NPC1 and HE1) can cause the disorder. NPC1 is the best characterized of the proteins produced by these two genes; it is a multi-pass membrane protein that contains a SCAP-

like cholesterol-sensing motif. Several observations implicate NPC1 in cholesterol transport to and from caveolae. Progesterone mimics the cholesterol transport defects exhibited by NPC1-defective cells (Butler *et al*., 1992). A subset of the NPC1-positive vesicle population in cells is positive for caveolin-1 (Garver *et al*., 2000). The cholesterol content of caveolae in NPC1$^{-/-}$ cells is reduced 3-fold relative to caveolae from matched wild-type cells (Garver *et al*., 2002). The lower caveolae cholesterol is accompanied by an increased expression of caveolin-1 (Garver *et al*., 1999, 2002). Finally, the decreased level of cholesterol in NPC1 neuronal membranes has been linked to the ERK activation and tau phosphorylation (Sawamura *et al*., 2001). We have also observed that the basal level of pERK in human NPC1 fibroblasts is markedly higher than normal fibroblasts (data not shown). These observations biochemically and genetically link NPC1 to the transport of cholesterol between caveolae and other cellular membranes. Exactly how ERK1/2 controls the function of NPC1 remains to be established.

Materials and methods

Materials

Rabbit pAb phospho-ERK1/2 IgG that recognizes pERK1/2 when it is phosphorylated on both Thr202/Tyr204 was from New England Biolabs (Beverly, MA). mAb pERK1/2 IgG that recognizes either monophosphorylated (Thr202) or the di-phosphorylated forms of ERK1/2 was from Sigma (St Louis, MO). Rabbit pAb pSAPK IgG was from Promega (Madison, WI). Rabbit pAb SAPK1 IgG, murine pERK2–GST, pSAPK1α-HIS, mAb and pAb HA-tag IgG, pAb ERK1/2 IgG, mAb ERK2 IgG, rabbit pAb and mAb PP2A C subunit, A subunit and B subunit IgG, mAb pY IgG (4G10), purified human blood cell PP2A, Ser/Thr phosphatase assay kit 1, sheep pAb phospho-ERK1/2 IgG that recognizes both monophosphorylated (Tyr204) and the di-phosphorylated ERK1/2 all were from UBI (Lake Placid, NY). Glutathione–agarose and protein G and A PLUS-agarose beads were from Santa Cruz Biotechnology, Inc. (Santa Cruz, CA). Okadaic acid, PD98059 and U0126 were from Biomol (Plymouth, PA). Sodium orthovanadate was from Aldrich (Milwaukee, WI). Methyl-β-cyclodextrin was from Sigma. Centricon filters from Millipore Corp. (Bedford, MA). Superdex 200 HR 10/30 column, MonoQ HR 5/5 column and the automatic fast protein liquid chromatography station were from Amersham Pharmacia Biotech (Piscataway, NJ). Protease inhibitor cocktail set III was from CalBiochem (La Jolla, CA). The cDNA for HePTP in a pEF/HA vector was a kind gift from Dr Thomas Mustelin (La Jolla, CA).

Cell culture, transfection and cholesterol depeletion

Cells were cultured at 37°C in a humidified atmosphere containing 5% CO_2. Normal human fibroblasts were grown in low-glucose Dulbecco's modified Eagle's medium (DMEM) (Invitrogen) and HeLa cells were grown in high-glucose DMEM (Invitrogen). Human fibroblasts were cultured 8–10 days before each experiment. HeLa cells were cultured until confluent. All media contained 10% fetal bovine serum (FBS), 100 U/ml penicillin and 100 U/ml streptomycin. HeLa cells were transfected with a cDNA coding for HA-HePTP using LipofectAMINE PLUS reagent according to the manufacturer's instructions. Cells were acutely depleted of cholesterol by incubating them in the presence of 1% CD for 30–60 min at 37°C. Control cells for the cholesterol depletion experiments were incubated in the presence of either serum-free DMEM alone or a mixture of 1% CD and 100 μg/ml cholesterol for 30–60 min at 37°C.

In vitro phosphatase assay

Cells were washed three times with cold phosphate-buffered saline (PBS) and then homogenized in 1 ml of buffer A (50 mM Tris–HCl pH 7.5, 0.1 mM EGTA, 0.1% β-mercaptoethanol) containing 0.1 mM phenylmethylsulfonyl fluoride (PMSF), 1 μg/ml pepstatin A, 1 μg/ml aprotinin and 1 μg/ml leupeptin using a 2 ml tissue grinder fitted with Teflon pestle. The lysates were centrifuged for 10 min at 1000 *g* at 4°C to remove nucleus and unbroken cells. The supernatant was then centrifuged at 200 000 *g* for 45 min at 4°C to remove membranes. The supernatant fraction (30 μg), designated as cytosol, was mixed with 100 ng of pERK2–GST in 300 μl of buffer A and incubated for the indicated time at 30°C. In some experiments the pERK2–GST was isolated from the mixture by adding 20 μl of preblocked glutathione–agarose beads and pelleting the beads. In others all of the protein in the mixture was precipitated with 7% trichloroacetic acid (TCA). The TCA precipitate and the GST fusion protein on the beads were dissolved in buffer B (62.5 mM Tris–HCl pH 6.8, 10% glycerol, 2% SDS, 1% β-mercaptoethanol, 5 μg/ml bromphenol blue), separated by gel electrophoresis, transfered to immobilon-P membrane and immunoblotted to detect pERK2. The same procedure was used to assay for dephosphorylation of pSAPK1α. Phosphatase assays on fractionated cytosol were carried out the same way, substituting the whole cytosol with the indicated fractions. To determine the phosphatase activity in the immunoisolates, each pellet was mixed with 100 ng pERK2–GST in 100 μl of buffer A plus PMSF, pepstatin, aprotinin and leupeptin as described above. The samples were rotated at 30°C for the indicated time then mixed with 20 μl of 6× buffer B, boiled for 5 min, separated by gel electrophoresis and immunoblotted with the indicated antibody.

Isolation of ERK phosphatase activity

Normal human fibroblasts or HeLa cells were scrapped into cold PBS. The 50–100, 100 mm dishes of human fibroblasts or 20, 150 mm dishes of HeLa cells were washed twice with cold PBS and homogenized using a nitrogen bombing at 400 p.s.i. for 15 min on ice in 4 ml cold buffer C (Tris 10 mM pH 7.5, NaCl 150 mM, EDTA 0.1 mM, plus 1/1000 of the protease inhibitor cocktail set). The lysate was first centrifuged for 10 min at 1000 *g* at 4°C and centrifuged for 45 min at 200 000 *g*, 4°C to remove membranes. The cytosol supernatant was loaded on a MonoQ HR5/5 column, which was installed on an automatic fast protein liquid chromatography station. After extensive washing with five bed volumes (5 ml) of 250 mM NaCl in 10 mM Tris at pH 7.5, the proteins bound to the column were eluted using a 250–450 mM linear gradient of NaCl pH 7.5, at a flow rate of 0.5 ml/min. The pERK phosphatase activity in each fraction was measured as described. The peak activity in fractions between 350 and 380 mM NaCl were pooled and concentrated using a 30 kDa centricon. The concentrated material was resuspended in 0.5 ml buffer C and put on a Superdex 200 gel filtration column that was calibrated with a high molecular weight gel filtration calibration kit. Fractions were eluted in buffer C at a flow rate of 0.5 ml/min. The pERK phosphatase activity in each fraction was measured as described above.

Immunoisolation procedure

Fractions 10 to 13 from the Superdex 200 column were pooled and concentrated with a 100 kDa centricon filter. mAb $PP2A_C$ IgG (15 μg) or an irrelevant mAb IgG designated 2001 (15 μg) were mixed with 150 μg sample protein in 300 μl buffer C. After rotating overnight at 4°C, the sample was mixed with 40 μl (1:1 slurry) of pre-blocked protein G (for mAb) or protein A (for pAb) conjugated to PLUS-agarose beads, and the rotation was continued for 2 h. The beads were then separated from the supernatant and washed five times in buffer C. The supernatant fraction and pellet was saved for analysis.

In some experiments we used the method of Tanoue *et al*. (2000) to isolate the HePTP/PP2A complex. Cells were homogenized in hypotonic buffer D (20 mM HEPES pH 7.4, 2 mM EGTA, 2 mM $MgCl_2$ and protease inhibitors) according to the method of Tanoue *et al*. (2000). The lysate was first centrifuged at 1000 *g* for 10 min to remove unbroken cells and the nucleus. The supernatant was then centrifuged at 20 000 *g* for 10 min. The high-speed supernatant was adjusted to a protein concentration of 0.5 mg/ml and used for immunoprecipitation. A 300 μl sample was mixed with 5 μg of the indicated antibody and incubated with continuous rotation overnight at 4°C. A/G PLUS-agarose (20 μl) was added to each sample and the rotation was continued for another 2 h at 4°C. After three washes with buffer E (10 mM Tris–HCl pH 7.5, 150 mM NaCl, 0.1 mM EDTA, 0.1% Triton X-100), the proteins on the beads was eluted from the beads by boiling in SDS sample buffer, separated on SDS–PAGE and immunoblotted with the indicated antibody.

Other methods

Caveolae were isolated by the method of Smart *et al*. (1995). Blue native PAGE was used according to the method of Yang *et al*. (2002). Protein was measured using the Bradford method. The serine/threonine phosphatase activity in the PP2A immunoprecipitates was measured using 400 μM R-K-pT-I-R-R peptide and a Malachite Green phosphatase assay kit according to the manufacturer's instructions.

Acknowledgements

We would like to thank Dr Yiheng Hao and Meifang Zhu for their valuable technical assistance, and Brenda Pallares for administrative assistance. This work was supported by grants from the National Institutes of Health (HL 20948, GM 52016, AG 18883) and the Perot Family Foundation.

References

Alessi,D.R., Gomez,N., Moorhead,G., Lewis,T., Keyse,S.M. and Cohen,P. (1995) Inactivation of p42 MAP kinase by protein phosphatase 2A and a protein tyrosine phosphatase, but not CL100, in various cell lines. *Curr. Biol.*, **5**, 283–295.

Anderson,R.G. (1998) The caveolae membrane system. *Annu. Rev. Biochem.*, **67**, 199–225.

Brown,M.S. and Goldstein,J.L. (1997) The SREBP pathway: regulation of cholesterol metabolism by proteolysis of a membrane-bound transcription factor. *Cell*, **89**, 331–340.

Butler,J.D. *et al*. (1992) Progesterone blocks cholesterol translocation from lysosomes. *J. Biol. Chem.*, **267**, 23797–23805.

Camps,M., Nichols,A., Gillieron,C., Antonsson,B., Muda,M., Chabert,C., Boschert,U. and Arkinstall,S. (1998) Catalytic activation of the phosphatase MKP-3 by ERK2 mitogen-activated protein kinase. *Science*, **280**, 1262–1265.

Camps,M., Nichols,A. and Arkinstall,S. (2000) Dual specificity phosphatases: a gene family for control of MAP kinase function. *FASEB J.*, **14**, 6–16.

Cobb,M.H. (1999) MAP kinase pathways. *Prog. Biophys. Mol. Biol.*, **71**, 479–500.

Fielding,C.J. and Fielding,P.E. (1997) Intracellular cholesterol transport. *J. Lipid Res.*, **38**, 1503–1521.

Furuchi,T. and Anderson,R.G. (1998) Cholesterol depletion of caveolae causes hyperactivation of extracellular signal-related kinase (ERK). *J. Biol. Chem.*, **273**, 21099–21104.

Garver,W.S. and Heidenreich,R.A. (2002) The Niemann–Pick C proteins and trafficking of cholesterol through the late endosomal/lysosomal system. *Curr. Mol. Med.*, **2**, 485–505.

Garver,W.S., Hossain,G.S., Winscott,M.M. and Heidenreich,R.A. (1999) The Npc1 mutation causes an altered expression of caveolin-1, annexin II and protein kinases and phosphorylation of caveolin-1 and annexin II in murine livers. *Biochim. Biophys Acta*, **1453**, 193–206.

Garver,W.S., Heidenreich,R.A., Erickson,R.P., Thomas,M.A. and Wilson,J.M. (2000) Localization of the murine Niemann–Pick C1 protein to two distinct intracellular compartments. *J. Lipid Res.*, **41**, 673–687.

Garver,W.S., Krishnan,K., Gallagos,J.R., Michikawa,M., Francis,G.A. and Heidenreich,R.A. (2002) Niemann–Pick C1 protein regulates cholesterol transport to the *trans*-Golgi network and plasma membrane caveolae. *J. Lipid Res.*, **43**, 579–589.

Gronda,M., Arab,S., Iafrate,B., Suzuki,H. and Zanke,B.W. (2001) Hematopoietic protein tyrosine phosphatase suppresses extracellular stimulus-regulated kinase activation. *Mol. Cell. Biol.*, **21**, 6851–6858.

Groom,L.A., Sneddon,A.A., Alessi,D.R., Dowd,S. and Keyse,S.M. (1996) Differential regulation of the MAP, SAP and RK/p38 kinases by Pyst1, a novel cytosolic dual-specificity phosphatase. *EMBO J.*, **15**, 3621–3632.

Gustavsson,J. *et al*. (1999) Localization of the insulin receptor in caveolae of adipocyte plasma membrane. *FASEB J.*, **13**, 1961–1971.

Ito,J., Nagayasu,Y., Kato,K., Sato,R. and Yokoyama,S. (2002) Apolipoprotein A-I induces translocation of cholesterol, phospholipid and caveolin-1 to cytosol in rat astrocytes. *J. Biol. Chem.*, **277**, 7929–7935.

Kabouridis,P.S., Janzen,J., Magee,A.L. and Ley,S.C. (2000) Cholesterol depletion disrupts lipid rafts and modulates the activity of multiple signaling pathways in T lymphocytes. *Eur. J. Immunol.*, **30**, 954–963.

Lange,Y. (1994) Cholesterol movement from plasma membrane to rough endoplasmic reticulum. Inhibition by progesterone. *J. Biol. Chem.*, **269**, 3411–3414.

Liu,P., Wang,P., Michaely,P., Zhu,M. and Anderson,R.G. (2000) Presence of oxidized cholesterol in caveolae uncouples active platelet-derived growth factor receptors from tyrosine kinase substrates. *J. Biol. Chem.*, **275**, 31648–31654.

Maxfield,F.R. and Wustner,D. (2002) Intracellular cholesterol transport. *J. Clin. Invest.*, **110**, 891–898.

Murata,M., Peranen,J., Schreiner,R., Wieland,F., Kurzchalia,T.V. and Simons,K. (1995) Vip21/caveolin is a cholesterol-binding protein. *Proc. Natl Acad. Sci. USA*, **92**, 10339–10343.

Okamoto,Y., Ninomiya,H., Miwa,S. and Masaki,T. (2000) Cholesterol oxidation switches the internalization pathway of endothelin receptor type A from caveolae to clathrin-coated pits in Chinese hamster ovary cells. *J. Biol. Chem.*, **275**, 6439–6446.

Pettiford,S.M. and Herbst,R. (2000) The MAP-kinase ERK2 is a specific substrate of the protein tyrosine phosphatase HePTP. *Oncogene*, **19**, 858–869.

Ponting,C.P. and Aravind,L. (1999) START: a lipid-binding domain in StAR, HD-ZIP and signalling proteins. *Trends Biochem. Sci.*, **24**, 130–132.

Pulido,R., Zuniga,A. and Ullrich,A. (1998) PTP-SL and STEP protein tyrosine phosphatases regulate the activation of the extracellular signal-regulated kinases ERK1 and ERK2 by association through a kinase interaction motif. *EMBO J.*, **17**, 7337–7350.

Roth,G., Kotzka,J., Kremer,L., Lehr,S., Lohaus,C., Meyer,H.E., Krone,W. and Muller-Wieland,D. (2000) MAP kinases Erk1/2 phosphorylate sterol regulatory element-binding protein (SREBP)-1a at serine 117 *in vitro*. *J. Biol. Chem.*, **275**, 33302–33307.

Rothberg,K.G., Heuser,J.E., Donzell,W.C., Ying,Y.S., Glenney,J.R. and Anderson,R.G. (1992) Caveolin, a protein component of caveolae membrane coats. *Cell*, **68**, 673–682.

Sawamura,N., Gong,J.S., Garver,W.S., Heidenreich,R.A., Ninomiya,H., Ohno,K., Yanagisawa,K. and Michikawa,M. (2001) Site-specific phosphorylation of tau accompanied by activation of mitogen-activated protein kinase (MAPK) in brains of Niemann–Pick type C mice. *J. Biol. Chem.*, **276**, 10314–10319.

Saxena,M., Williams,S., Tasken,K. and Mustelin,T. (1999) Crosstalk between cAMP-dependent kinase and MAP kinase through a protein tyrosine phosphatase. *Nat. Cell Biol.*, **1**, 305–311.

Shiozuka,K., Watanabe,Y., Ikeda,T., Hashimoto,S. and Kawashima,H. (1995) Cloning and expression of PCPTP1 encoding protein tyrosine phosphatase. *Gene*, **162**, 279–284.

Smart,E.J., Ying,Y.S., Mineo,C. and Anderson,R.G. (1995) A detergent-free method for purifying caveolae membrane from tissue culture cells. *Proc. Natl Acad. Sci. USA*, **92**, 10104–10108.

Smart,E.J., Ying,Y., Donzell,W.C. and Anderson,R.G. (1996) A role for caveolin in transport of cholesterol from endoplasmic reticulum to plasma membrane. *J. Biol. Chem.*, **271**, 29427–29435.

Sontag,E. (2001) Protein phosphatase 2A: the Trojan Horse of cellular signaling. *Cell. Signal.*, **13**, 7–16.

Sontag,E., Fedorov,S., Kamibayashi,C., Robbins,D., Cobb,M. and Mumby,M. (1993) The interaction of SV40 small tumor antigen with protein phosphatase 2A stimulates the map kinase pathway and induces cell proliferation. *Cell*, **75**, 887–897.

Tanoue,T., Adachi,M., Moriguchi,T. and Nishida,E. (2000) A conserved docking motif in MAP kinases common to substrates, activators and regulators. *Nat. Cell Biol.*, **2**, 110–116.

Uittenbogaard,A. and Smart,E.J. (2000) Palmitoylation of caveolin-1 is required for cholesterol binding, chaperone complex formation and rapid transport of cholesterol to caveolae. *J. Biol. Chem.*, **275**, 25595–25599.

Uittenbogaard,A., Everson,W.V., Matveev,S.V. and Smart,E.J. (2002) Cholesteryl ester is transported from caveolae to internal membranes as part of a caveolin–annexin II lipid–protein complex. *J. Biol. Chem.*, **277**, 4925–4931.

Yang,T., Espenshade,P.J., Wright,M.E., Yabe,D., Gong,Y., Aebersold,R., Goldstein,J.L. and Brown,M.S. (2002) Crucial step in cholesterol homeostasis: sterols promote binding of SCAP to INSIG-1, a membrane protein that facilitates retention of SREBPs in ER. *Cell*, **110**, 489–500.

Zanke,B., Suzuki,H., Kishihara,K., Mizzen,L., Minden,M., Pawson,A. and Mak,T.W. (1992) Cloning and expression of an inducible lymphoid-specific, protein tyrosine phosphatase (HePTPase). *Eur. J. Immunol.*, **22**, 235–239.

Zhang,F., Strand,A., Robbins,D., Cobb,M.H. and Goldsmith,E.J. (1994) Atomic structure of the MAP kinase ERK2 at 2.3 Å resolution. *Nature*, **367**, 704–711.

Zhou,B., Wang,Z.X., Zhao,Y., Brautigan,D.L. and Zhang,Z.Y. (2002) The specificity of extracellular signal-regulated kinase 2 dephosphorylation by protein phosphatases. *J. Biol. Chem.*, **277**, 31818–31825.

Received January 23, 2003; revised March 18, 2003; accepted March 28, 2003